Int. J. Electrochem. Sci., 12 **(2017)** 9502 – 9511, doi: 10.20964/2017.10.54

International Journal of ELECTROCHEMICAL SCIENCE
www.electrochemsci.org

Development of a Graphene-Based Aptamer Sensor for Electrochemical Detection of Serum ECP Levels

Zhitao Wang[1], *Jun Yang*[2] *and Lin Gui*[3*]

[1] Department of Pediatrics, Wuchang Hospital, Wuhan, Hubei, 430063, P.R. China
[2] Department of Pediatrics, Xiangaoxin Hospital, Xian, Shanxi, 710075, P.R. China
[3] Department of Paediatrics, Maternal and Child Health Hospital of Hubei Province, Wuhan, Hubei, 430070, P. R. China
[*]E-mail: guilin_vivi@163.com

Received: 17 June 2017 / *Accepted:* 11 August 2017 / *Published:* 12 September 2017

The eosinophil cationic protein (ECP) is the biological marker for bronchial eosinophil inflammation, and it can be detected in serological levels to objectively predict the activity and severity of asthma in children. This work reports a facile electrochemical aptasensor without labels for the detection of ECP using a glassy carbon electrode (GCE) modified by Au nanoparticles dotted with a graphene (GNPs/GR) nanocomposite film. The ECP-aptamer interactions were studied using ferricyanide as the electrochemical probe. The terminal GNPs/GR layer displayed an acceptable current for ECP determination. The peak current variation of ferricyanide was linearly related to the ECP concentration (0.01 μM - 10 μM), and the limit of detection (LOD) was 4 nM.

Keywords: Eosinophil cationic protein; Aptamer sensor; Graphene; Electrochemical determination; Children asthmatic attack

1. INTRODUCTION

Asthma is a chronic inflammatory disease of the airways, and eosinophil cells play a vital part in asthma [1]. The pathogenesis of this inflammatory disease can be better understood by observing the behaviour of the bronchoalveolar lavage and lung biopsies [2-4]. There are several proteins in eosinophil granules, including a major basic protein, eosinophil cationic protein (ECP), eosinophil-derived neurotoxin and eosinophil peroxidase. The aforementioned cells and the corresponding granule products are potential markers of the inflammation severity [5-7]. Among the eosinophil proteins, ECP has been the most extensively investigated. In bronchial asthma and other eosinophil-involved diseases, including atopic dermatitis, rhinitis, autoimmune diseases and parasitic infections, there is an

increase in ECP [8, 9]. Viral and bacterial infections also show an increase in the ECP level [10]. While it is toxic to parasites, ECP is not bactericidally active. ECP is a neurotoxin [11], and ECP has a pronounced effect on clotting through the neutralization of anticoagulant activity after binding to heparin [12]. Bronchial asthma has attracted the most attention. Investigations have observed a correlation between the ECP levels in sputum, blood and bronchoalveolar lavage and the inflammation severity [13-17]. Kalaajieh and Hoilat investigated the ECP levels during an outbreak of asthma in children [18]. The ECP level of all the asthmatics during the outbreak was remarkably higher than that of the control group. There was a pronounced decrease in the ECP levels two weeks after the exacerbation was resolved. Asthmatics with severe attacks had the highest ECP levels, while those with moderate/mild attacks showed no statistical variation. At the 2 week follow-up, the ECP levels in patients with moderate/mild attacks were comparable to that of the control levels but the levels continuously increased in the severe attack subgroup. The ECP levels in the serum showed no obvious correlation with the eosinophil count, blood oxygen saturation or peak expiratory rate.

Therefore, detecting the ECP level is important for clinical applications. The focus of the current techniques for ECP level detection has been primarily on the CAP-system (CAP-ECP-FEIA pharmacia). After being covalently coupled to immuno CAP, anti-ECP reacts with the ECP in the serum of a patient. After washing, a complex is formed via the addition of monoclonal anti-ECP to betagalactosidase. This was followed by washing the unbound anti-ECP conjugated with the betagalactosidase, and the bound complex was incubated with 4-menthylum-belliferyl-beta-D-galactosidase as the fluorogenic substrate. The elute fluorescence measurement was performed after termination of the reaction, and the fluorescence was in direct proportion to the ECP concentration in the serum specimen. All the measurements were performed in duplicate. The ECP standard pattern was recorded over a range of 2 - 200 μg/L. However, the preparation and measurements for this technique are rather time-consuming.

Aptamers are single-stranded, short, artificial DNA/RNA oligonucleotides that are selected in vitro via a systematic evolution of ligands by exponential enrichment (SELEX) [19, 20]. The specific features of aptamers contribute to their successful competition with antibodies as biorecognition elements for biosensors. They can be selected and bound to extensive targets, such as small molecules, proteins or even whole cells, with a high specificity and affinity [21-24]. The aptamers are thermally stable and can be reused. Through the introduction of functional groups, aptamers can be easily modified for their immobilization and determination. Hence, aptamer-based sensors have wide applications for the determination of organic molecules, cancer cells and diverse proteins. Electrochemical aptamer-based sensors are extensively used since they are sensitive, simple, and inexpensive, and they have rapid responses. Diverse materials have been introduced for electrode modification to achieve enhanced sensitivity in electrochemical aptasensors. Graphene (GR) is a two-dimensional sheet of carbon atoms bonded through sp^2 hybridization [25-32], and since it was discovered by Geim et al., it has been an attractive material because it has low manufacturing costs, good mechanical strength, desirable thermal and electrical conductivities and a large specific area [33, 34]. Moreover, gold nanoparticle-dotted graphene (GNPs/GR) has the potential to have synergistic effects on electrochemical features and promote the sensitivity of a sensor, and it has gained

increasingly widespread attention as an enhanced sensing material for electrochemical sensor fabrication [35].

This study developed a facile and sensitive electrochemical aptasensor to detect ECP levels based on a desirable current response from GNPs/GR nanocomposites. The Au nanoparticles and thiol termini on the aptamers formed thiol–gold (S–Au) bonds, which led to the immobilization of the anti-ECP aptamer on the glassy carbon electrode (GCE). A ferricyanide electrochemical probe was used to investigate the interaction between the anti-ECP aptamer and the target, and the interaction was then monitored via differential pulse voltammetry (DPV) and cyclic voltammetry (CV).

2. EXPERIMENTS

2.1. Chemicals

Graphene oxide (GO) was commercially available from Nanjing Xianfeng Nano Co. Ltd. The synthetic anti-ECP aptamer was commercially available from Sangon Biotechnology Co. Ltd. Chloroauric acid ($HAuCl_4$) was commercially available from Aladdin Reagent Co. Ltd. Tris-(2-carboxyethyl) phosphine hydrochloride (TCEP), 6-mercapto-1-hexanol (MCH) and eosinophil cationic protein (ECP) were commercially available from Sigma–Aldrich. All other chemicals were of analytical reagent grade and were used without further purification. Ultrapure water commercially available from a Millipore water purification system ($\geqslant$18 M Ω, Milli-Q Millipore) was used throughout the tests.

2.2. Preparation of the graphene-based aptasensor

The aptasensor preparation consisted of the GCE pretreatment, the immobilization of the GNPs/GR nanocomposite film, and the self-assembly of the anti-ECP aptamer. After successive polishing with 1.0, 0.3, and 0.05 μm Al_2O_3 slurries on chamois leather, the GCE was completely rinsed with doubly distilled water until its surface was mirror-like. This was followed by ultrasonic washing in absolute ethanol and water for 5 min. After this, the GCE was dried under a nitrogen stream at ambient temperature. The second step began with uniformly dropping the GO suspension (5.0 μL, 1.0 mg/mL) onto a freshly smoothed GCE surface. In addition, the yielded solvent was evaporated at ambient temperature, and this was followed by a complete rinsing with ultrapure water to remove the excess GO. GO was electrochemically reduced on the electrode surface in the N_2 purged PBS solution (pH 8.0) at a working potential of −1.2 V (vs Ag/AgCl) for 800 s. This was followed by immersing the modified electrode in a chloroauric acid solution (0.1 mM) containing 0.5 M sulphuric acid with a constant potential of −0.25 V for 30 s to electrodeposit the GNPs. After rinsing with ultrapure water, the modified electrode was dried at ambient temperature. Finally, the anti-ECP aptamer (anti-ECP) was self-assembled onto the GNPs/GR/GCE. The anti-ECP aptamer was processed prior to use. First, the denaturation of the anti-ECP aptamer was achieved via heat treatment at 90 °C for 10 min, and this was followed by fast cooling at 4 °C for 15 min and incubation at 25 °C for 5 min. During this process, the most stable conformation for the renaturation of aptamer was obtained, which is a prerequisite for

it to bind to the target molecule. This was followed by the reduction of the anti-ECP aptamer solution in TCEP (2 mM) for 60 min to cleave the disulphide bonds. The GNPs/GR/GCE was placed in a solution containing MCH and the anti-ECP at varied concentrations at 4 °C for 16 h under 100% moisture-saturated conditions to immobilize the aptamer. Eventually, the deionized water was used to rinse the anti-ECP/MCH/GNPs/GR/GCE.

2.3. Characterizations

A CHI 440A electrochemical workstation was used for the electrochemical assays. A traditional triple-electrode configuration was used throughout the tests, and it consisted of a glassy carbon electrode (GCE) as the working electrode, a platinum counter electrode, and an Ag/AgCl (sat. KCl) reference electrode. The anti-ECP/MCH/GNPs/GR/GCE was immersed into a binding buffer solution containing ECP at a given concentration for 0.5 h at ambient temperature to form the anti-ECP and target complexes, which were then completely washed with the binding buffer solution to remove the unbound ECP. The $K_3[Fe(CN)_6]/K_4[Fe(CN)_6]$ containing a 0.1 M KCl solution was used throughout the electrochemical assays. Cyclic voltammetric (CV) assays were conducted at potentials ranging from −0.1 to 0.6 V (scan rate: 50 mV/s). In terms of the electrochemical differential pulse voltammetry (DPV) assays, the voltage scanning range, pulse height, step height and frequency were −0.1 to 0.7 V, 50 mV, 50 mV and 5.0 Hz, respectively.

3. RESULTS AND DISCUSSION

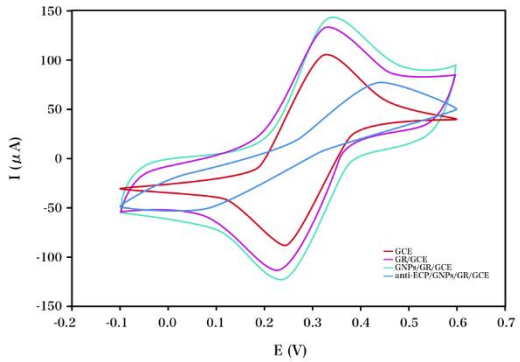

Figure 1. CV of the original GCE, GR/GCE, GNPs/GR/GCE, and anti-ECP/GNPs/GR/GCE in an aqueous solution containing $[Fe(CN)_6]^{3-/4-}$ (5.0 mM) and KCl (0.1 M).

The CV measurements confirmed the immobilization of each functionalized layer on the GCE surface. Figure 1 displays the CVs of the varied electrodes in the $[Fe(CN)_6]^{3-/4-}$solution (5.0 mM). A significant redox peak was not observed for the original GCE. In contrast, the GR/GCE displayed a significant current response due to the pronounced increase in the electrode conductivity and the facilitated electron-exchange via the GR/GCE. There was a further increase in the peak current for the

GNPs/GR/GCE, which indicated that this nanocomposite has synergistic effects on the electrochemical features. One possible explanation for the aptasensor background signal is the non-specific adsorption caused by the high concentration of the binding buffer on the electrode surface [36]. A decrease in the redox peak current for the anti-ECP/GNPs/GR/GCE was observed, which suggested that the electron exchange in the redox probe could be blocked by the aptamers that decorated the electrode surface.

We optimized the aptamer and MCH concentrations over the ranges of 0.1 to 10 μM and 0.5 to 10 μM, respectively, to achieve the maximal sensitivity. Figure 2A shows the relative DPV peak current variations in the presence and absence of ECP at a constant MCH concentration and varied aptamer concentrations. It was found that only 1 μM of ECP resulted in a significant peak current change, while the same concentration of the other three interfering agents resulted in slight emissions [37]. Figure 2B shows the relative DPV peak current variations in the presence and absence of ECP with a constant aptamer concentration and varied MCH concentrations (0.5, 1.0, 2.0, 5.0 and 10 μM). The best sensitivity was obtained with an aptamer concentration of 1.0 μM and an MCH concentration of 2.0 μM. Hence, the optimized concentrations of the aptamer and MCH were 1.0 μM and 2.0 μM, respectively, and these concentrations were used in the following tests.

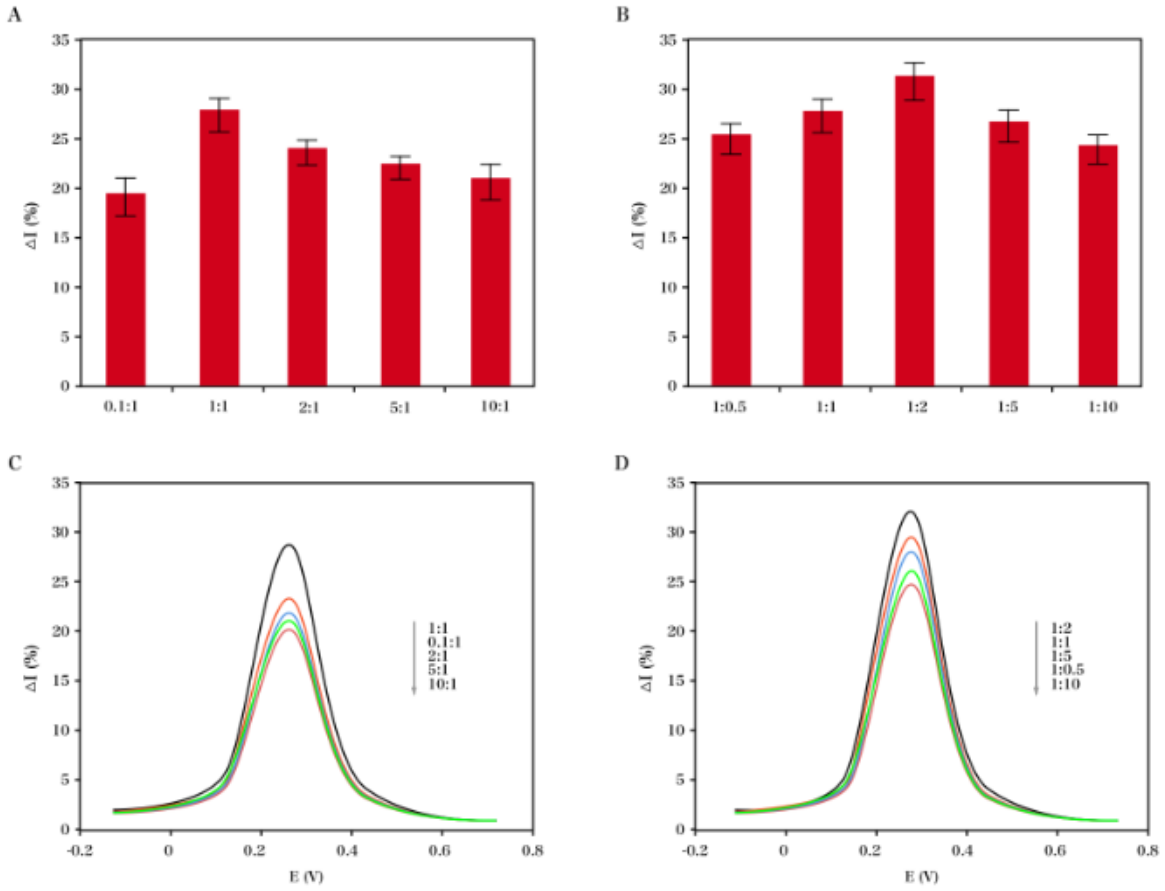

Figure 2. The relative DPV peak current variations observed for the aptamer/MCH optimization. (A) The five plots characterizing measurements with the aptamer (0.1, 1.0, 2.0, 5.0 and 10 μM) and 1.0 μM of the immobilized MCH. (B) The results obtained from immobilization with the aptamer (1.0 μM) and 0.5, 1.0, 2.0, 5.0 and 10 μM of MCH.

We also explored the aptamer/MCH incubation time to obtain a desirable sensitivity for the as-prepared aptasensor. Figure 3A shows the incubation time dependence of the response of the DPV peak current in the presence and absence of 1.0 μM of ECP. As the incubation time increased, there was an increase in the DPV peak current variation, which became steady at 12 h. The lack of variation after 12 h suggested the saturation of the aptamer/MCH on the decorated GCE surface. Therefore, the optimal incubation time was fixed at 12 h. In addition, the ECP detection time was another important parameter that significantly affected the DPV peak current variation. Hence, we also investigated the dependence of the ECP detection time on the current increase to obtain the optimal ECP detection time. Upon the addition of 1.0 μM of ECP, there was an increase in the current and a plateau after 0.5 h (Figure 3B), which suggested the aptamer/ECP complexes saturated the surface of the electrode. Therefore, the detection time for ECP was optimized at 0.5 h.

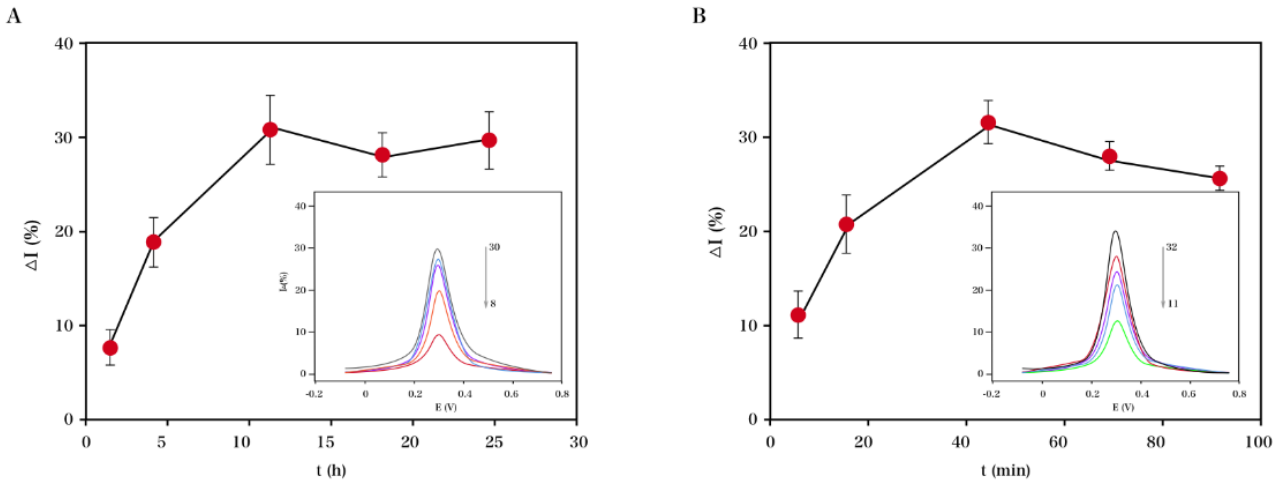

Figure 3. Relative DPV peak current variations observed through the optimization of (A) the incubation time for the aptamer/MCH and (B) the detection time for ECP.

The DPV responses of the proposed aptasensors incubated with ECP at varying concentrations under the optimum conditions were characterized herein. As the ECP concentration increased from 0 μM to 10 μM, there was a decrease in the DPV peak current (Figure 4A). In addition, as shown in Figure 4B, the ECP determination was characterized via a logarithm linear calibration pattern ($I=0.94887\log_{(concentration)} + 16.83562$) with a correlation coefficient (R^2) of 0.994 at 0.01 μM - 10 μM range and a limit of detection (LOD) of 0.004 μM (S/N = 3). To allow for a realistic comparison to previous reports, the characteristics of different analytical methods for ECP are summarized in Table 1. For the ECP concentrations from 0.01 μM to 100 μM, the current variations were ca. 10 − 45% (Figure 4B). There was a decrease in the current at lower concentrations. However, this was possibly not a result of the ECP binding to the aptamer because the background signal variation was also ca. 5%. The current variations with the addition of 100 μM ECP and 10 μM ECP were similar, and this was possibly because the anti-ECP aptamer (1 μM) immobilized on the surface of the modified electrode was saturated with ECP (over 10 μM).

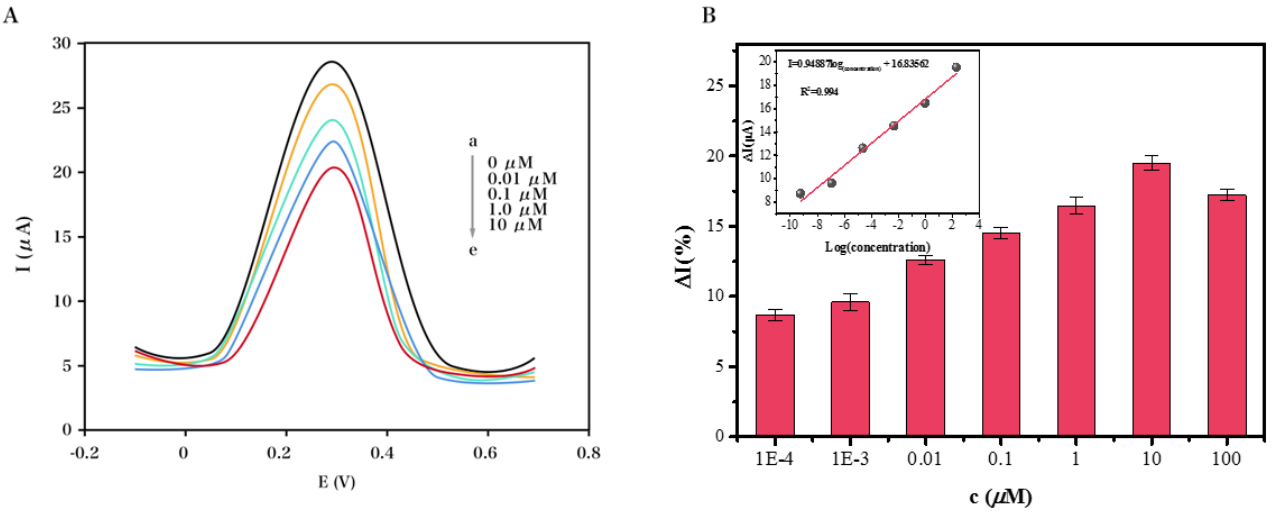

Figure 4. (A) DPV patterns of the aptasensor incubated with different concentrations of ECP (a–e: the BPA concentrations: 0, 0.01, 0.1, 1.0 and 10 μM). (B) Linear relationship between the peak current variation (Δ*I*) and the ECP concentrations.

Table 1. Comparison of the major characteristics of analytical methods used for the detection of ECP.

Electrode	Linear detection range	Detection limit	Reference
Electrophoresis	0.1 - 1μM	0.02 μM	[38]
Enzyme immunoassay	15–1000 ng	-	[39]
Aptamer/MCH	0.01 - 10 μM	0.004 μM	This work

In addition to a desirable sensitivity, an aptasensor should be specific for an analyte at varied concentrations. The DPV peak current variation was detected before and after the addition of ECP and interference agents, including glucose, uric acid and ascorbic acid. As shown in Figure 5, the obvious peak current variation only appeared with the addition of 1 μM of ECP, and the same concentrations of the three interference agents resulted in insignificant emissions. However, the prepared aptasensor showed a performance comparable to that of other aptasensors in real assays [40, 41], which indicated that the developed aptasensor can be applied for the analysis of EPC.

The ECP (1.0 μM) detection was repeated to investigated the reproducibility of the as-prepared aptasensor. After each determination, the as-prepared electrode was refreshed under 10 consecutive CV sweeps in a range of 0.0 to 0.5 V at 50 mV/s in 0.1 M $NH_3 \cdot H_2O$–NH_4Cl buffer (pH 9.3) to remove any possible adsorbents. The results indicated that the six assays were favourably reproducible, and the relative standard deviation (RSD) was 3.8%. A regenerated electrode surface could be used consecutively fifteen times without any behaviour deterioration (RSD: 4.3%), which suggested that the sensor was stable. The responses of the six aptasensors from the same batch to ECP (1.0 μM) were detected to study the preparation reproducibility, and an RSD of 3.7% was obtained, which indicated the proposed aptasensor was reproducible for the ECP determination. Moreover, the obtained aptasensor was utilized to analyse ECP in three serum samples. The results of the ECP content

determination in these samples are shown in Table 2. As shown, the aptasensor had an excellent performance for ECP detection in the serum samples.

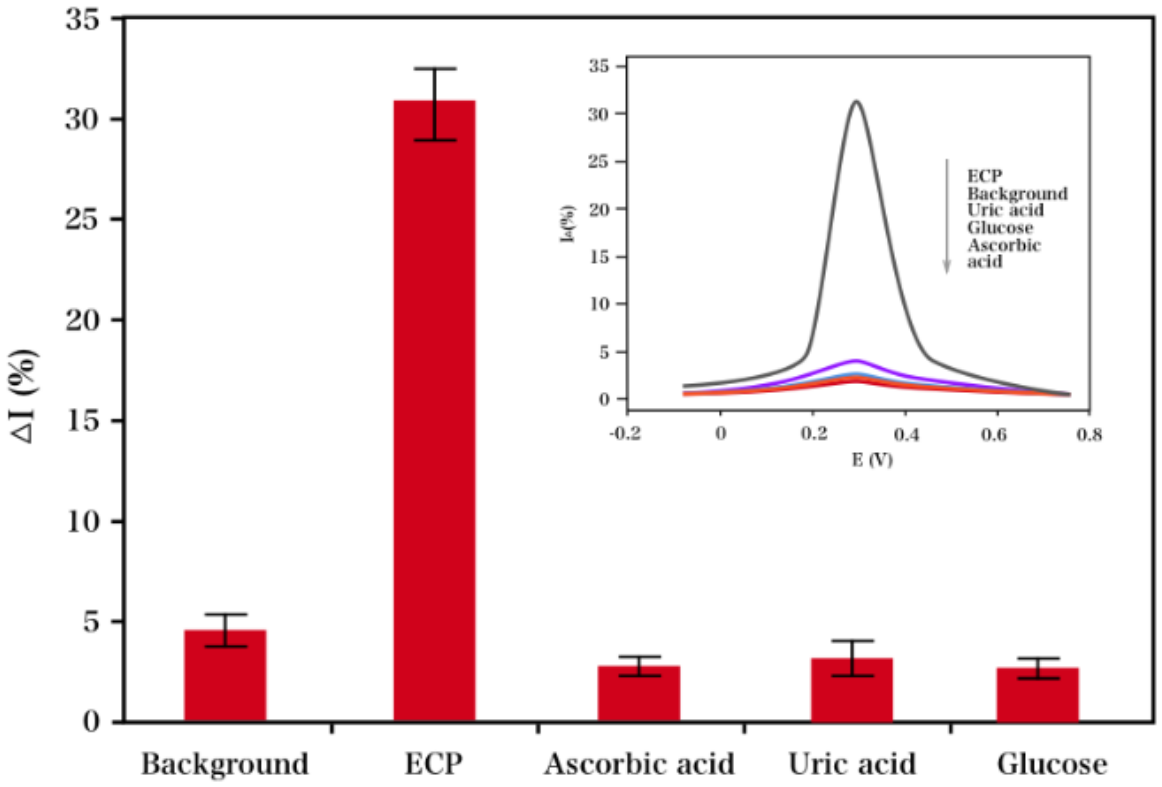

Figure 5. A comparison of the ECP specificity (1.0 μM) of the aptasensor in the presence of interference agents: glucose, uric acid and ascorbic acid.

Table 2. The contents and recoveries of aptasensor for ECP determination (n=3).

Sample	Added (μM)	Found (μM)	ELISA result (μM)	Recovery (%)	RSD (%)
1	0.1	0.107	0.109	107	1.7
2	0.5	0.491	0.502	98.2	3.2
3	2.0	2.104	2.100	105.2	2.9

4. CONCLUSIONS

This work reported the fabrication of an electrochemical aptasensor without a label for ECP detection. After direct immobilization onto an electrode decorated with the GNPs/GR nanocomposite film, the aptamer worked to capture ECP. The determination was based on the ECP binding-induced current decrease. Conventionally, the determination of ECP has been achieved using electrochemical

aptasensors based on target-induced conformational variations. In comparison, this proposed aptasensor uses a less complex detection system.

ACKNOWLEDGEMENT
This work was supported by grants from the Hubei Province health and family planning scientific research project (No.WJ2017M132) and Hubei maternal and child health care research topic (No.2016-07).

References

1. J. Bousquet and F.B. Michel, *Allergy*, 47 (1992) 129.
2. J. Bousquet, P. Chanez, J. Lacoste, G. Barnéon, N. Ghavanian, I. Enander, P. Venge, S. Ahlstedt, J. Simony-Lafontaine and P. Godard, *N. Engl. J. Med.*, 323 (1990) 1033.
3. S. Ahlstedt, J. Enander, C. Peterson, S. Rak and P. Venge, *Pharmaceutical Medicine*, 6 (1992) 99.
4. A. Tonnel, P. Gosset and I. Tillie-Leblond, *International Archives of Allergy and Immunology*, 124 (2001) 267.
5. L. Prin, *Revue Francaise d Allergologie et d Immunologie Clinique*, 36 (1996) 889.
6. A. Niimi, R. Amitani, K. Suzuki, E. Tanaka, T. Murayama and F. Kuze, *Clinical & Experimental Allergy*, 28 (1998) 233.
7. A. Niimi and H. Matsumoto, *Current Opinion in Pulmonary Medicine*, 5 (1999) 111.
8. M. Kägi, H. Joller-Jemelka and B. Wüthrich, *Dermatology*, 185 (1992) 88.
9. F. Tischendorf, N. Brattig, M. Lintzel, D. Büttner, G. Burchard, K. Bork and M. Müller, *Tropical Medicine & International Health*, 5 (2000) 898.
10. M. Karawajczyk, K. Pauksen, C.G.B. Peterson, E. Eklund and P. Venge, *Clinical & Experimental Allergy*, 25 (1995) 713.
11. R. Garofalo, J. Kimpen, R. Welliver and P. Ogra, *The Journal of Pediatrics*, 120 (1992) 28.
12. A. Björk, P. Venge and C. Peterson, *Allergy*, 55 (2000) 442.
13. J. Bousquet, P. Chanez, J.Y. Lacoste, I. Enander, P. Venge, C. Peterson, S. Ahlstedt, F. Michel and P. Godard, *Journal of Allergy and Clinical Immunology*, 88 (1991) 649.
14. P. Venge, *Respiratory Medicine*, 89 (1995) 1.
15. J. Fauquert, G. Beaujon, M. Héraud, M. Doly and A. Labbé, *Revue Française D'allergologie et d'immunologie Clinique*, 37 (1997) 227.
16. E. Grebski, J. Wu, B. Wüthrich and T.C. Medici, *Journal of Investigational Allergology & Clinical Immunology*, 9 (1998) 82.
17. N. Ishigaki, C. Masuhara, K. Sakamaki, Y. Ishikawa, K. Ohta, R. Koike, K. Mikuni, H. Haruna and S. Awa, *Arerugi*, 49 (2000) 1093.
18. W. Kalaajieh and R. Hoilat, *Revue Française d'Allergologie et d'Immunologie Clinique*, 41 (2001) 529.
19. A. Ellington and J. Szostak, *Nature*, 346 (1990) 818.
20. C. Tuerk and L. Gold, *Science*, 249 (1990) 505.
21. G. Bang, S. Cho and B. Kim, *Biosensors and bioelectronics*, 21 (2005) 863.
22. C. Huang, Y. Huang, Z. Cao, W. Tan and H. Chang, *Anal. Chem.*, 77 (2005) 5735.
23. M. Stojanovic and D. Landry, *Journal of the American Chemical Society*, 124 (2002) 9678.
24. D. Wilson and J. Szostak, *Annual Review of Biochemistry*, 68 (1999) 611.
25. C. Bosch-Navarro, Z. Laker, J. Rourke and N. Wilson, *Phys Chem Chem Phys*, 17 (2015) 29628.
26. J. Huang, Z. Xie, Z. Xie, S. Luo, L. Xie, L. Huang, Q. Fan, Y. Zhang, S. Wang and T. Zeng, *Anal. Chim. Acta.*, 913 (2016) 121.
27. P. Bollella, G. Fusco, C. Tortolini, G. Sanzò, G. Favero, L. Gorton and R. Antiochia, *Biosensors and Bioelectronics*, 89 (2017) 152.

28. S. Xu, Y. Zhang, K. Dong, J. Wen, C. Zheng and S. Zhao, *Int. J. Electrochem. Sci*, 12 (2017) 3443.
29. S. Asif, S. Khan and A. Asiri, *Journal of the Taiwan Institute of Chemical Engineers*, (2017)
30. H. Zhou, W. Wang, P. Li, Y. Yu and L. Lu, *Int. J. Electrochem. Sci*, 11 (2016) 5197.
31. S. Bhardwaj, P. Yadav, S. Ghosh, T. Basu and A. Mahapatro, *ACS Applied Materials & Interfaces*, 8 (2016) 24350.
32. T. Chen, L. Tang, F. Yang, Q. Zhao, X. Jin, Y. Ning and G. Zhang, *Analytical Letters*, 49 (2016) 2223.
33. L. Al-Mashat, K. Shin, K. Kalantar-zadeh, J. Plessis, S. Han, R.W. Kojima, R. Kaner, D. Li, X. Gou and S. Ippolito, *J Phys Chem C*, 114 (2010) 16168.
34. W. Hong, H. Bai, Y. Xu, Z. Yao, Z. Gu and G. Shi, *J Phys Chem C*, 114 (2010) 1822.
35. L. Ruiyi, X. Qianfang, L. Zaijun, S. Xiulan and L. Junkang, *Biosensors and Bioelectronics*, 44 (2013) 235.
36. L. Zhou, J. Wang, D. Li and Y. Li, *Food Chemistry*, 162 (2014) 34.
37. P. Kalinowski, A. Strzelczyk, L. Wozniak, G. Jasinski and P. Jasinski, *Measurement Science and Technology*, 25 (2014) 025101.
38. E. Carreras, E. Boix, H. Rosenberg, C. Cuchillo and M. Nogués, *Biochemistry*, 42 (2003) 6636.
39. C. Reimert, P. Venge, A. Kharazmi and K. Bendtzen, *Journal of Immunological Methods*, 138 (1991) 285.
40. S. Liu, X. Xing, J. Yu, W. Lian, J. Li, M. Cui and J. Huang, *Biosensors and Bioelectronics*, 36 (2012) 186.
41. Q. Cao, H. Zhao, L. Zeng, J. Wang, R. Wang, X. Qiu and Y. He, *Talanta*, 80 (2009) 484.